J. Fluid Mech. (1971), vol. 47, part 1, pp. 33–49
Printed in Great Britain

The effect of atmospheric conditions on plume rise

By P. R. SLAWSON AND G. T. CSANADY
University of Waterloo, Ontario

(Received 14 June 1968 and in revised form 9 June 1970)

The buoyant rise of chimney plumes is discussed for relatively large distances from the source, where atmospheric turbulence is the dominant cause of mixing (rather than turbulence due to the plume's own upward motion). A simple theory is developed which shows a number of different shapes plumes can have under different atmospheric conditions (particularly in an unstable environment).

Experimental data are then presented, which were collected in the field near Toronto, with reasonably detailed supporting information on the atmospheric temperature structure. These (and earlier results) often show quite complex plume behaviour at large distances from the source, which can, however, be readily understood in terms of the simple theory presented.

Introduction

Hot gases discharged from a chimney into the atmosphere drift upward owing to their buoyancy at a speed usually rather smaller than wind speed. The flow pattern in the resulting nearly horizontal plume is then very similar to that in a turbulent 'line thermal'. The upward drift of plumes and thermals depends critically on their growth by entrainment of ambient fluid, as has been made clear in a classic paper by Morton, Taylor & Turner (1956).

The Morton *et al.* paper deals with plumes and thermals in quiescent surroundings in which case the turbulence causing the entrainment is generated by the plume's own motion. When the environment is already turbulent (as the atmosphere is) both the 'self generated' and the 'environmental' turbulence presumably contribute to growth. Relatively simple conditions may be expected to result if one or the other dominates. In Csanady (1965) the atmospheric-turbulence dominated phase of a line-thermal was briefly discussed for the case of neutral stratification. This could be subdivided into two subphases characterized by growth being due respectively (*a*) to eddies in the inertial subrange and (*b*) to the energy containing eddies. The rate of growth in case (*a*) is very much more vigorous.

In an earlier paper (Slawson & Csanady 1967, to be referred to as S & C) we have further discussed the dynamics of plume motion in the three phases, 'initial' (self-generated turbulence determines growth), 'intermediate' (atmospheric eddies in the inertial subrange determine growth) and 'final' (energy containing eddies of atmospheric turbulence determine growth). We have shown that the extension of the Morton *et al.* theory to these three phases led to essentially the same predictions as the line-thermal theory presented in Csanady

(1965). We have also presented some observational evidence collected with particular care and demonstrated that the *mean* path of plumes in neutral surroundings behaves according to theory in the *initial* phase. There was no intermediate phase in evidence in those observations, but the final phase behaviour again seemed to follow the theory, although the evidence for this was not conclusive because it covered some rather special conditions only.

Several other contributions to the buoyant plume problem appeared in the literature since S & C went to press (Moore 1966; Briggs 1969; Bringfelt 1969; Hoult, Fay & Forney 1969) and reasonable concensus emerged on the mean path of hot plumes in the 'initial' phase, under neutral and stable atmospheric stratification. Non-neutral conditions are modelled theoretically by assuming the atmospheric potential temperature gradient to be constant.

While such progress is gratifying in a subject beset by much past confusion, some important observed facts remain unexplained. Even if we disregard the influence of the more obvious atmospheric inhomogeneities (concentrated shear layers and inversions), the initial phase theory cannot account for the peculiar shape of plumes in unstable surroundings (we have presented some examples of these in S & C with a very crude qualitative explanation); nor is the long-term behaviour of plumes in near-neutral conditions well documented or understood.

In the present paper we therefore address ourselves mainly to the behaviour of plumes beyond the 'initial' phase, where the evidence indicates strong influences from an interplay of stratification and atmospheric turbulence (the latter insofar as it affects plume growth). The extension of the three-phase theory introduced in Csanady and developed in S & C leads to a number of theoretical predictions, which seem to explain some of the complex observed phenomena reported in S & C. We also report here some further field observations, many being supported by fairly detailed atmospheric temperature profiles to 300 m observed by means of kite-borne radio-sondes. Such temperature profiles are quite helpful in the interpretation of the observed results. When this information is available, the extended simple theory appears to account for many observed complexities of plume rise.

Extended simple theory

The by-now well-established 'initial phase' theory of buoyancy-dominated plume rise rests on the following assumptions: (i) The plume rise is caused mainly by buoyancy. This assumption restricts the validity of the theory to plumes from large heat sources and even then excludes a small portion of the plume immediately downwind of the chimney where initial momentum is important. (ii) The wind speed is approximately constant with height in the region where the plume is rising. (iii) The dominant dispersing agent (for heat and vertical momentum) is the plume's 'self-generated' turbulence, i.e. that due to the bodily vertical motion of the plume (this restricts the theory to an 'initial' phase of motion, before environmental turbulence becomes dominant). (iv) The potential temperature gradient of the atmosphere is constant with height, again in the region where the plume is rising (it can be positive, negative or zero).

The theory has been developed with these assumptions by Moore (1966) and others, and it fairly successfully correlates field observations on observed mean plume paths at moderate distances from the source. Particularly good results are obtained for *stable* atmospheric conditions (Briggs 1969; Bringfelt 1969). By changing or replacing assumptions (i) and (ii) the theory may be extended to momentum dominated plumes and more complex conditions but we shall not be concerned with this.

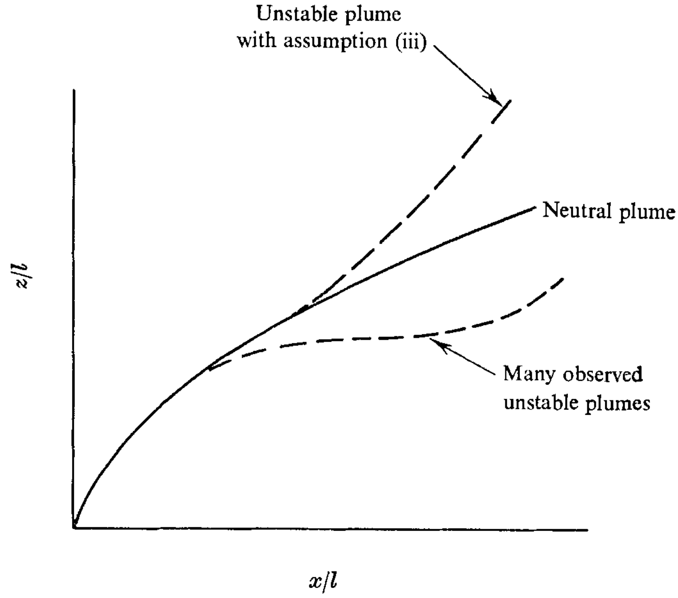

FIGURE 1. Theory and experiment on unstable plumes.

The most conspicuous departures from the above theory occur with plumes observed under unstable conditions: some (but not all) plumes remain decisively below the theoretical predictions, as illustrated in figure 1. We have already reported this phenomenon in S & C. Also, even plumes in nearly neutral surroundings do not appear to follow the $\frac{2}{3}$ power law at large enough distances, although evidence on this point is meagre. In order to explain such effects, an extension may be made to simple approximate theory if we replace assumption (iii) above by: (iii*a*) Atmospheric turbulence becomes the dominant plume-dispersing agent beyond a certain transition point.

The consequences of this assumption have been worked out in S & C for neutral plumes, and Bringfelt (1969) also uses it in his discussion, mainly in establishing the range of validity of the theory based on assumptions (i)–(iv). In the following we will show that the complex observed mean paths of plumes in unstable and strongly turbulent surroundings can be explained in terms of an extended simple theory based on assumptions (i), (ii), (iii*a*) and (iv).

Governing equations

Assumption (iii$a$) leads to an equation expressing the rate of growth of a plume in terms of atmospheric turbulence parameters. Because the growth of a chimney plume is a problem in 'relative' diffusion, the rate of growth depends on the size of the cloud, as long as the latter is small compared to the 'energy containing eddies' of the environmental turbulence. Thus we are led to three different mass-balance equations characterizing 'initial', 'intermediate' and 'final' phases of plume growth. The vertical momentum equation, and the energy (density defect) equation remains more or less as already introduced in Morton *et al.*

mass:

$$U\,dR^2/dx = 2\alpha|w|\,R \quad \text{(initial phase) (self-generated turbulence);} \tag{1a}$$

$$U\,dR^2/dx = 2a_1\epsilon^{\frac{1}{3}}R^{\frac{4}{3}} \quad \text{(intermediate phase) (eddies in inertial subrange);} \tag{1b}$$

$$U\,dR^2/dx = 2a_2 vL \quad \text{(final phase) (energy containing eddies);} \tag{1c}$$

momentum: $$U\,d(R^2w)/dx = R^2b; \tag{2}$$

density defect: $$U\,d(R^2b)/dx \doteq -R^2wN^2. \tag{3}$$

The above equations are based on the assumption of a 'top-hat' profile (constant w, b within plume). A somewhat more general approach is to assume arbitrary, but self-similar distributions, which introduces constants of order unity into (2) and (3). We shall not pursue this complication here.

Above U is the mean wind speed, w, $b = g\,\Delta\rho/\rho$ and R are vertical velocity, buoyant acceleration and radius of the plume respectively. The constant α is the 'entrainment constant' for the initial phase, while a_1, a_2 are corresponding constants relating turbulence parameters to plume growth (v = r.m.s. turbulent velocity, L = length scale of the energy-containing eddies, ϵ = rate of energy dissipation per unit mass).

The effect of stability enters through the parameter

$$N^2 = -\frac{g}{\rho_1}\frac{d\rho_a}{dz} \simeq \frac{g}{T_1}\frac{d\theta_a}{dz},$$

where g is acceleration of gravity, θ_a, ρ_a and T_1 are the potential temperature, density and absolute temperature, density changes being assumed small compared to a reference density ρ_1. As mentioned before, N will be assumed constant. In stable conditions, N^2 is positive, and N is the Brunt–Väisälä frequency, while in unstable and neutral conditions, N^2 is negative and zero respectively.

Equations (2) and (3) are to be solved with the initial conditions

$$\left.\begin{aligned} R^2w &= 0 \\ \text{and} \qquad R^2b &= F/U \end{aligned}\right\} \quad \text{at} \quad x = 0, \tag{4}$$

where F is the initial 'flux of buoyancy' variable, $F = gQ/\pi\rho_g c_p T_1$ with Q heat flux at the chimney, ρ_g gas density, c_p specific heat.

With these initial conditions, (2) and (3) have the solution

$$R^2w = (lU^2/N)\sin(Nx/U), \tag{5}$$

$$R^2b = lU^2\cos(Nx/U), \tag{6}$$

where l is a buoyancy length scale defined by

$$l = F/U^3. \tag{7}$$

Equations (5) and (6) are applicable in all three phases of motion in any conditions of linear thermal stratification (including neutral stratification).

The initial phase

Equation (5) shows that negative vertical velocities will occur in a stable atmosphere, hence the absolute value $|w|$ appears in (1a), expressing the fact than entrainment always leads to plume growth (this formulation was suggested by a referee). It may be pointed out here that the entrainment assumption expressed in (1a) is likely to be a poor model of plume growth near the point on the plume path where $w = 0$. Ignoring this difficulty, however, and assuming that N is real (stable conditions), (1a) and (5) yield for the '*initial phase*' of plume growth, using $R = 0$ at $x = 0$ as a simplified initial condition:†

$$R^3 = [3\alpha lU^2/N^2]\,[(2n-1)+(-1)^n\cos(Nx/U)] \quad (n = 1, 2, \ldots), \tag{8}$$

where n is an integer such that $(n-1)\pi U/N \leqslant x \leqslant n\pi U/N$. The equation for the mean path is now obtained by substituting (8) into (5), noting that

$$dz/dx = w/U \quad \text{and taking} \quad z = 0 \quad \text{at} \quad x = 0. \tag{9}$$

Thus after integration we find

$$\frac{z}{l} = C_n + (-1)^{n+1}\left(\frac{3U^2}{\alpha^2l^2N^2}[(2n-1)+(-1)^n\cos(Nx/U)]\right)^{\frac{1}{3}}, \tag{10}$$

where
$$C_n = \left(\frac{3U^2}{N^2\alpha^2l^2}\right)^{\frac{1}{3}}\sum_{p=1}^{n}(-1)^p(2p-2)^{\frac{1}{3}}$$

for the range of x specified in (8). The resulting initial phase plume path shows damped oscillations in the vertical with circular frequency N. The plume levels off asymptotically at the height of

$$z/l = 1{\cdot}53(U^2/N^2\alpha^2l^2)^{\frac{1}{3}}. \tag{11}$$

The constant 1·53 has been arrived at by a numerical evaluation of (10) to large x, and agrees with the value quoted by Bringfelt (1969).

The maximum rise, which occurs when $x = \pi U/N$, is $z/l = 1{\cdot}82(U^2/N^2\alpha^2l^2)^{\frac{1}{3}}$. Thus the final rise is 16 % less than the maximum. Also, momentum is a maximum at $x = \pi U/2N$ where buoyancy is zero, giving a significant momentum 'overshoot' to the plume for

$$\pi U/2N \leqslant x \leqslant \pi U/N.$$

† The finite initial size of the plume may be taken into account by placing a 'virtual' origin some distance below and upstream of the source.

Near the origin, $x \ll U\pi/N$, the plume path is found by expanding the cosine term in (10),

$$z/l = (3/2\alpha^2)^{\frac{1}{3}}\,(x/l)^{\frac{2}{3}}, \tag{12}$$

which is the same as the neutral plume path arrived at in S & C.

In *unstable* conditions, when N^2 is negative, (5) and (6) solve with (1*a*) to give for the initial phase

$$R^3 = \frac{3\alpha l U^2}{N^2}\left(\cosh\frac{|N^2|^{\frac{1}{2}}x}{U} - 1\right) \quad (0 \leqslant x \leqslant x_1). \tag{13}$$

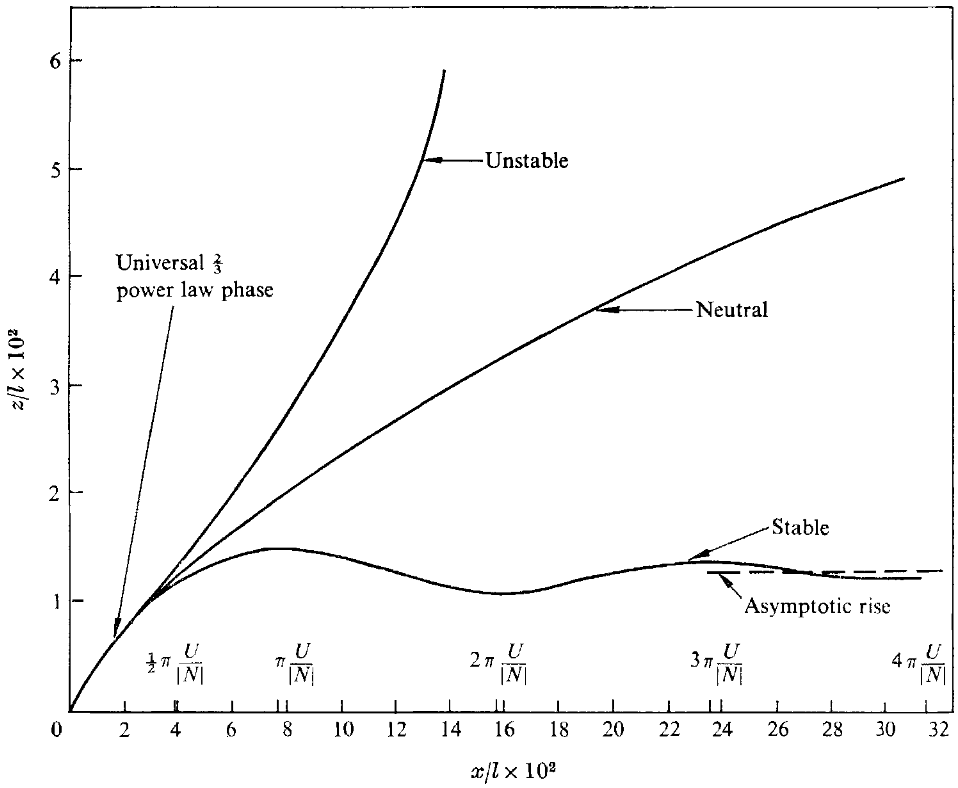

Figure 2. Typical 3 phase behaviour of buoyant plumes under neutral, unstable, and stable atmospheric conditions.

Substituting (13) into (5) and again using the relation (9) we have, after integration, the mean path given by

$$\frac{z}{l} = \left[\left(\frac{3U^2}{|N^2|\,\alpha^2 l^2}\right)\left(\cosh\frac{|N^2|^{\frac{1}{2}}x}{U} - 1\right)\right]^{\frac{1}{3}}. \tag{14}$$

The character of this solution is already illustrated in figure 1. As in stable conditions, (14) also reduces to the $\frac{2}{3}$ law of neutral conditions given by (12) for $x \ll \pi U/|N^2|^{\frac{1}{2}}$. This is to be expected, because expanding either the cosine term in (10) or the hyperbolic cosine of (14), for small x, is equivalent to the expansion for small N. The solutions (10) and (14) are thus valid for all stable and unstable conditions including the limiting condition of neutral stability. The results of the first phase theory for all stability conditions are illustrated in figure 2. They may be summarized in the following simplifications: (1) Sufficiently close to the source the $\frac{2}{3}$ power law holds in all stability conditions. (2) Stable plumes level off at a well-defined height, possibly after a noticeable 'overshoot'. (3) Unstable plumes rise more or less exponentially after they depart from the universal $\frac{2}{3}$ law path.

Atmospheric turbulence dominated phases

Turning now to the *intermediate and final phases* of plume growth, where atmospheric turbulence is assumed to dominate the dispersion of the plume, we find that equations (1*b*) and (1*c*) may be integrated to give

$$R^2 = [R_1^{\frac{2}{3}} + 2a_1\epsilon^{\frac{1}{3}}(x-x_1)/3U]^3 \quad (x_1 \leqslant x \leqslant x_2), \tag{15}$$

and

$$R^2 = R_2^2 + 2a_2 vL(x-x_2)/U \quad (x \geqslant x_2), \tag{16}$$

where subscripts 1 and 2 denote the start of the second and third phases. From equations (5) and (9) we obtain the expression for the slope of the plume (in any phase, or under any linear stratification):

$$\frac{dz}{dx} = \frac{Ul}{R^2N}\sin\left(\frac{Nx}{U}\right). \tag{17}$$

The plume path for a specific phase may now be obtained by integrating (17), after substitution of R^2 from (5) and (6). However, some general conclusions may be derived at once.

In the intermediate phase the rate of plume growth is rapid and the plume slope generally decreases. Under unstable conditions $\sin(Nx/U)$ becomes $\sinh(|N^2|^{\frac{1}{2}}x/U)$ with the result that plume slope will grow indefinitely at sufficiently large x. However, the value of $|N^2|^{\frac{1}{2}}/U$ is often such that such an increase is not, in fact, observed. Under neutral conditions $UN^{-1}\sin(Nx/U)$ reduces to x, thus the slope is

$$dz/dx = lx/R^2. \tag{17a}$$

This also reduces sharply in the intermediate phase, but tends to a constant in the final phase. Under stable conditions there is a tendency to level off already in the initial phase: this is enhanced in the intermediate phase, somewhat reduced in the final phase.

The transition from the initial to the intermediate phase occurs when atmospheric turbulence of the inertial subrange takes over from the plume's self-generated turbulence as the principal mechanism for growth or dispersion. It, therefore, seems reasonable to equate the growth rates of the initial and intermediate phases in order to determine this transition 'point'. It is, of course, a gross simplification to imagine that such a transition takes place suddenly, but in the present state of the theory, a refinement would seem to be pointless. Thus, we postulate (as in S & C) that, at the transition point x_1, the 'entrainment velocity'

$\alpha|w|$ of the initial phase just becomes equal to the velocity scale of eddies of size R (i.e. that the right-hand sides of (1 *a*) and (1 *b*) just become equal). Thus

$$\alpha w_1 = a_1 \epsilon^{\frac{1}{3}} R_1^{\frac{1}{3}}, \tag{18}$$

where subscript 1 denotes transition point variables.

It will be sufficient to solve for the transition point x_1 for neutral conditions, in order to show its dependence on atmospheric parameters. From the initial phase, (8), (9) and (10), we have

$$R_1 = (\tfrac{3}{2}\alpha l)^{\frac{1}{3}} x_1^{\frac{2}{3}} \quad \text{and} \quad w_1 = U l^{\frac{1}{3}} (\tfrac{3}{2}\alpha)^{-\frac{2}{3}} x_1^{-\frac{1}{3}},$$

which, when substituted into (18), gives

$$x_1 = 0{\cdot}565 (\alpha l)^{\frac{2}{5}} (U/a_1 \epsilon^{\frac{1}{3}})^{\frac{9}{5}}. \tag{19}$$

It is a little more enlightning to express this result in terms of 'gustiness' v/U and scale (of turbulence) L, on writing $\epsilon = v^3/L$ (so that L is the 'dissipation' length scale: in view of having introduced the constant a_2 in (1 *c*), this is a permissible assumption). Also, introducing the definition of l, we have

$$x_1 = 0{\cdot}565 \frac{\alpha^{\frac{2}{5}}}{a_1^{\frac{9}{5}}} L \left(\frac{F}{U^3 L}\right)^{\frac{2}{5}} \left(\frac{U}{v}\right)^{\frac{9}{5}}. \tag{19a}$$

Although derived for the neutral case, (19 *a*) remains approximately valid for all stability conditions provided that the transition point occurs while the $\frac{2}{3}$ power law is still a good approximation to the mean plume path.

Equation (19 *a*) shows the expected result that (at constant wind speed and turbulence length-scale L) either a decrease in source strength and hence in self-generated turbulence, or an increase in atmospheric turbulence, will move the transition point closer to the source. At the same time, the non-dimensional abscissa x_1/l will also be proportional to $(L/l)^{\frac{3}{5}}$ and hence be relatively larger for smaller sources, or in high winds. Substituting into the expression for R_1 we find further for the transition radius for later use

$$\frac{R_1}{L} = A \left(\frac{l}{L}\right)^{\frac{3}{5}} \left(\frac{U}{v}\right)^{\frac{6}{5}} = A \left(\frac{F}{LUv^2}\right)^{\frac{3}{5}}, \tag{19b}$$

where $A = (\frac{3}{2})^{\frac{1}{3}}\, 0{\cdot}565^{\frac{2}{3}} \alpha^{\frac{3}{5}} a_1^{-\frac{6}{5}} =$ constant.

Similarly, by equating the growth rates for the intermediate and final phases, we find that

$$R_2 = \left[\frac{a_2 v L}{a_1 \epsilon^{\frac{1}{3}}}\right]^{\frac{3}{4}} = L \left(\frac{a_2}{a_1}\right)^{\frac{3}{4}} \left(\frac{v}{u}\right)^{\frac{3}{4}}, \tag{20}$$

which, with equations (15) and (19 *b*), gives

$$x_2 - x_1 = L \frac{3}{2a_1} \frac{U}{v} \left[\left(\frac{a_2}{a_1}\right)^{\frac{1}{2}} - A \left(\frac{l}{L}\right)^{\frac{3}{5}} \left(\frac{U}{v}\right)^{\frac{6}{5}}\right]. \tag{21}$$

Thus the distance over which the 'intermediate' phase would extend is, in order of magnitude, equal to length scale of turbulence L, divided by gustiness v/U or typically a few hundred metres. Furthermore, the possibility exists that the bracketed quantity in (21) becomes negligibly small or even negative, so that the 'intermediate' phase disappears altogether. This occurs when the ratio l/L is of the same order of magnitude as, or larger than v^2/U^2, a not uncommon set of circumstances for large power station chimneys at relatively low wind speeds. The quantity $l/L = F/LU^3$ varies rapidly with wind speed, while v^2/U^2 only changes slowly (although turbulence intensity depends on other conditions as well). Thus, for large heat sources, we derive the result that the 'initial' phase gives way directly to the 'final' phase at low speeds, or at low turbulence intensities, while a pronounced intermediate phase should exist at higher speeds or when turbulence is particularly intense. Because of the vigorous mixing in the intermediate phase, plumes should level off (change slope) rapidly in higher winds while they would retain an appreciable slope in low winds as they entered the 'final' phase, in which diffusion is less lively.

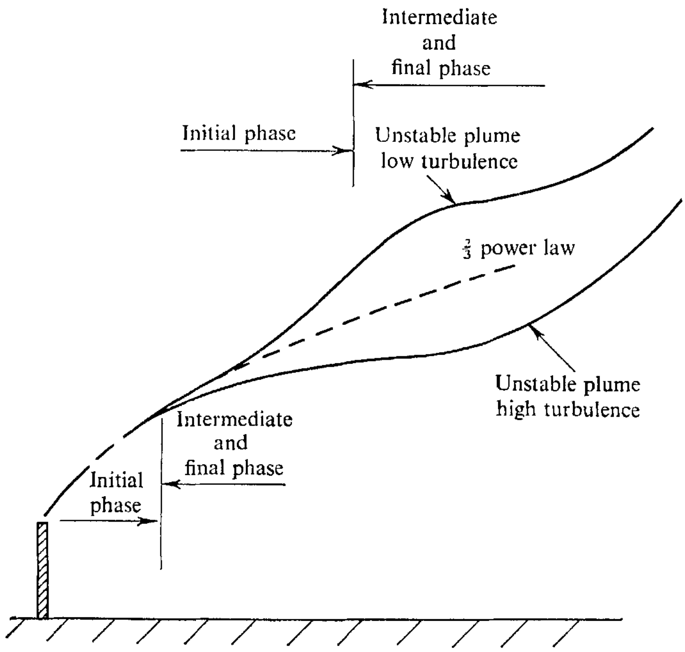

FIGURE 3. Two possibilities of unstable plume behaviour.

Equations (15) to (17) may be integrated numerically to give the plume path, once the initial conditions at the two transition points have been defined. In dealing with an actual plume, there is a certain amount of arbitrariness in the choice of these, so that there is little difficulty in producing a 'theoretical' curve following the observed one exceptionally well, while choosing very reasonable transition point conditions (such calculations have been presented by Slawson (1968)). The most interesting result in such calculations is obtained for *unstable* plumes: given the usual high turbulence level, the intermediate or final phase may start while there is still little departure from the $\frac{2}{3}$ power law in the initial phase. (Note that the 'initial phase' under unstable conditions contains a portion resembling a neutral plume at small distances, see (14).) Because the effect of atmospheric turbulence, once this takes over as the 'dominant' mixing mechanism, is to *increase* dilution compared to the mixing due to self-generated turbulence, the departure from the $\frac{2}{3}$ power law is, in this case, at first *downward.* Later, however, the instability of the atmosphere may dominate, cf. remark following (17). Thus we are led to a characteristic S-shaped curve, seen in many unstable plumes. On the other hand, when the turbulence intensity is not particularly high but instability is, the plume-slope may begin to increase in the later parts of the initial phase before a levelling-off takes place due to increased mixing in the intermediate or final phases. This then leads to a double S-shaped curve, because the instability still eventually dominates and produces an upward curvature. These two possibilities are illustrated in figure 3. This figure explains also why unstable plumes may be sometimes above, sometimes below the $\frac{2}{3}$ power law path, as reported from field observations in S & C.

Experimental technique

During the summer of 1967 another series of plume observations was carried out at the Lakeview (Toronto) power station, to supplement the 1965 data. The main improvement in technique was that a tethersonde provided the atmospheric temperature profile in the lowest 300 m. In addition, an effort was made to reduce errors of perspective further and at the same time to resolve more of the instantaneous plume on to film. To this end, the camera-transit levelling base, by which the film plane was maintained in the vertical, was further refined. In addition, two 35 mm single lens reflex cameras with colour and infra-red film were placed side by side and used to simultaneously photograph the instantaneous plume.

Two 150 m chimneys with 6 m internal diameters at the top, situated 75 m apart, discharged all of the flue gases during the experimental period. Two 300 MW turbine units per chimney operated at full load for the first two experiments while only one unit was operational on the second chimney for the remainder.

The stack gas exit parameters, mean wind speed at plume height and wind and turbulence data at a height of two meters were obtained as outlined in S & C. The plume was photographed every 2–5 min while temperature profiles to heights of approximately 300 m were simultaneously obtained. Two of the time-mean plume paths were obtained from 9 and 12 photographs while 18 to 31 were used to obtain the others. The temperature profile data were obtained by means of a Canadian Department of Transport chronometric tethersonde and associated receiving equipment.

The tethersonde was lifted aloft by means of specially designed stable kites. This simple, portable and inexpensive method of lifting the tethersonde was tested successfully in ground winds of 15 m/sec and to heights of 600 m. However, a flight ceiling of 300 m for the kites was imposed at the experimental site on account of nearby air traffic. The temperature profiles resulting from both ascent and descent of the tethersonde were averaged to give the final profile.

In 1967 there were two stacks operating during the experiments while only one was operational for the 1965 experiments. At a distance downwind of order 200 m the plumes from these two stacks were observed on two occasions to touch together. Upon an analysis of the photographs of these plumes, there was no discernible change in the rate of plume rise at or near where the two plumes touched.

A more detailed description of the experimental technique and equipment may by found in a report of limited circulation (Slawson 1968).

Results

The source and environment data are summarized in table 1. The average air temperature and gas exit velocity (w_0) for expts. 4–12 were 11·3 °C and 21 m/sec respectively. The flux of buoyancy in table 1 was calculated from $F = w_0 R_0^2 b_0$ where the zero subscript indicates source (stack exit) parameters.

Figure ...	4 (*a*)	4 (*b*)	4 (*c*)	4 (*d*)	4 (*e*)	4 (*f*)	4 (*g*)	4 (*h*)	4 (*h*)
Expt. no. ...	12	9	10	6	5	4	11	7	8
Wind speed at plume height (m/sec)	11·58	8·72	9·14	10·3	9·60	9·97	9·57	6·09	6·34
Gustiness									
Vertical G_v	0·085	0·074	0·133	0·092	0·071	0·040	0·117	0·062	0·074
Horizontal G_h	0·270	0·280	0·310	0·33	0·270	0·285	0·290	0·140	0·280
Temperature difference between stack gas at exit and ambient air ΔT (°C)	105·0	102·7	96·7	99·5	98·7	103·2	98·0	100·0	109·3
Mass flow of gas Mg (kg/h × 10^6)	1·92	1·92	1·93	1·93	1·94	1·89	1·89	1·93	1·92
Buoyant acceleration at chimney exit b_0 (m/sec^2)	3·54	3·51	3·23	3·44	3·38	3·63	3·29	3·57	3·84
Flux of buoyancy at the chimney F (m^4/sec^3)	667·1	655·0	610·1	631·7	627·4	642·9	606·7	658·4	721·5

TABLE 1. Lakeview generating station—plume rise observations

In one experiment (no. 12) the temperature distribution was neutral to 300 m and very probably above. The observed plume is shown in figure 4 (*a*) together with the temperature profiles. This plume behaves very much as the 1965 'neutral' plumes, consisting of a $\frac{2}{3}$ power law initial phase and an adjoining linear 'final' phase, with little or no discontinuity in slope at the breakup point, which may be interpreted to mean that no 'intermediate' phase was present. In the 1965 experiments a neutral stratification was inferred from circumstantial evidence and this experiment supports that inference. More specifically, by comparison with some other plumes discussed later a plume with these characteristics seems to exist in a neutral atmosphere when environmental turbulence is of relatively low intensity, as is also suggested by the theory above.

An interesting contrast is provided by expt. 9, figure 4 (*b*). On this day there was a strong lapse near the ground to some 100 m, then a nearly neutral layer as far as data show. One may expect strong thermal turbulence to have extended into the near-neutral layer above the unstable layer. The observed plume shows a very short $\frac{2}{3}$ power law region followed by a linear region of very low slope. The sharp change in slope in the neighbourhood of $x/l = 250$ may be interpreted as an 'intermediate phase' which should exist under the presumed high-turbulence conditions. The short initial phase, the presence of an intermediate phase, and the low final slope are all in accord with what theory suggests for the case of high environmental turbulence level, in neutral surroundings.

More or less the opposite situation is shown by the temperature profile for expt. 10, figure 4 (*c*): near neutral from the ground to a short distance above chimney-top (to $z/l \equiv 50$ or so), then moderately unstable, again neutral and then strongly unstable above 300 m or so. The plume behaves initially very much as in expt. 9: indeed to $x/l = 750$, the two plumes nearly coincide. Beyond this distance, however, the instability of the ambient air becomes evident in the plume of expt. 10 which embarks on something like an exponential rise until it reaches the strongly unstable layer, where it presumably encounters a much higher turbulence intensity. At still larger distances this plume should rise again, but it becomes invisible.

A more clear-cut example of an apparently exponential rise is shown in figure 4 (*d*) (expt. 6). Prior to this rise the plume falls *below* the $\frac{2}{3}$ power law, after making a fairly sudden turn, which suggests an 'intermediate' phase. No data were available for the temperature gradient over most of the plume rise in this instance.

The plume observed in expt. 5, figure 4 (*e*), is similar in general appearance to that of expt. 10, showing a well-marked intermediate phase and a following upward curvature. It is of some interest to compare this plume with one observed 2 years previously under very similar atmospheric conditions: the two plumes are evidently almost identical. The temperature profile over the plume rise region is unknown, but the strong scatter of lower level observations suggests high thermal turbulence, as postulated for expt. 10.

The plume of expt. 4, figure 4 (*f*), again behaves more or less as a neutral plume, but the transition point is close to the source and there is a fairly sudden change of slope, again indicating moderately high environmental turbulence. No temperature profile is available for this case.

The plume in expt. (11) behaved as a neutral plume until it hit a well-marked inversion indicated in the temperature profile figure 4 (*g*), where the plume levelled out.

The plumes in expts. 7 and 8 (figure 4 (*h*)) show behaviour known to be typical of stable atmospheric conditions (see, for example, Briggs 1969), in that they both fall below the $\frac{2}{3}$ power law and level out. The temperature profile for expt. 7 is not available, but that for expt. 8 shows slight stability above chimney-top, and rather more marked stability above 270 m. The plume levelled out at 420 m or so.

We may conclude that the mean path of hot chimney plumes in the 'real' atmosphere can have a complex shape indeed. Some of the complexities are clearly due to atmospheric inhomogeneities, such as inversion layers or strongly unstable layers. It should be equally clear from the above, however, that the influence of atmospheric turbulence on plume growth is also quite important in determining plume path. An 'initial phase' theory can only account for some of the simpler phenomena: the long-term behaviour of plumes is critically dependent on the effects of environmental turbulence. The simple theory presented above seems to provide a satisfactory framework for the understanding of much fascinating complexity in plume rise.

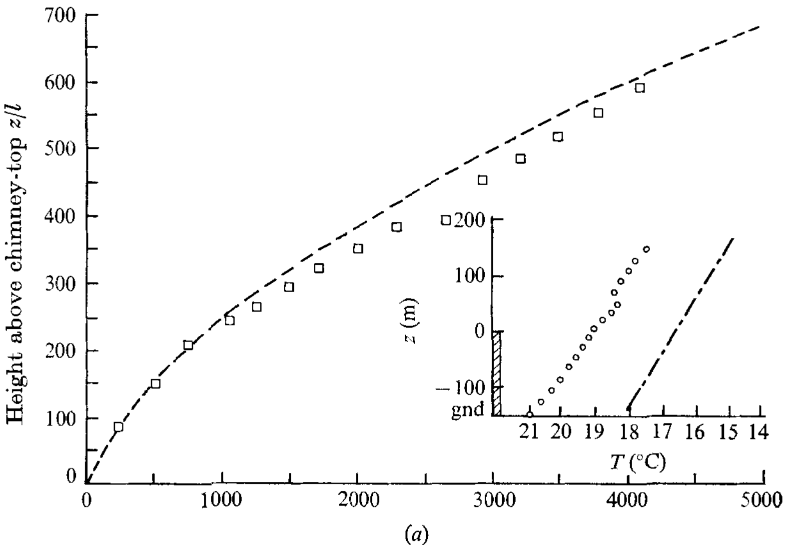

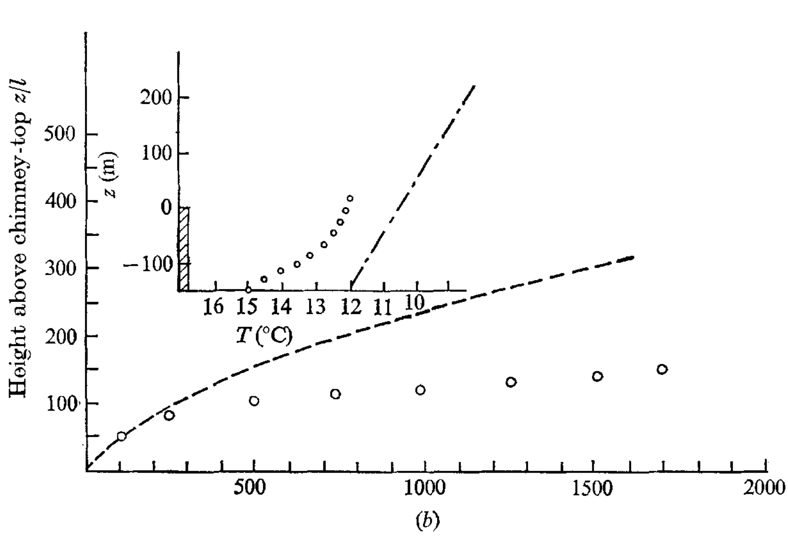

FIGURE 4 (a) and (b). For legend see p. 48.

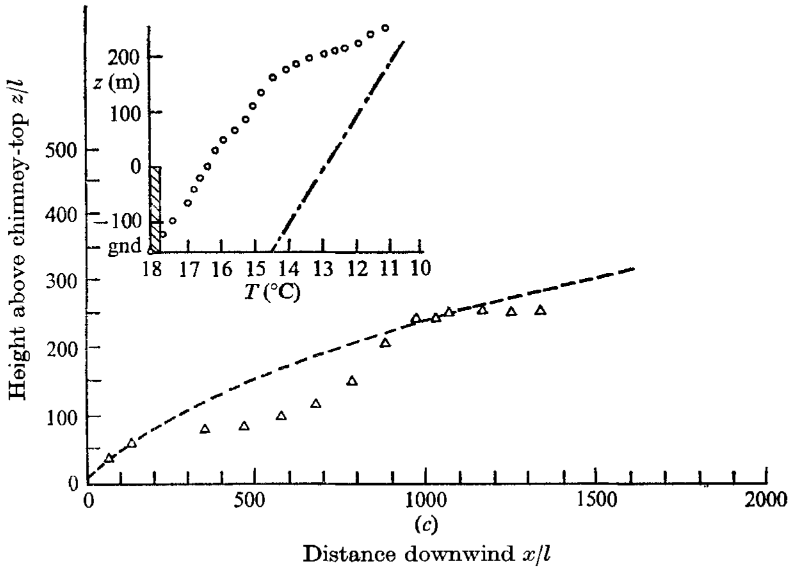

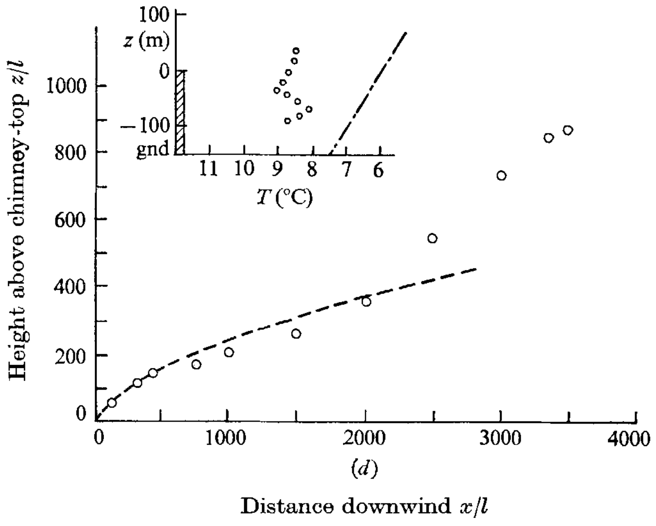

FIGURE 4 (c) and (d). For legend see p. 48.

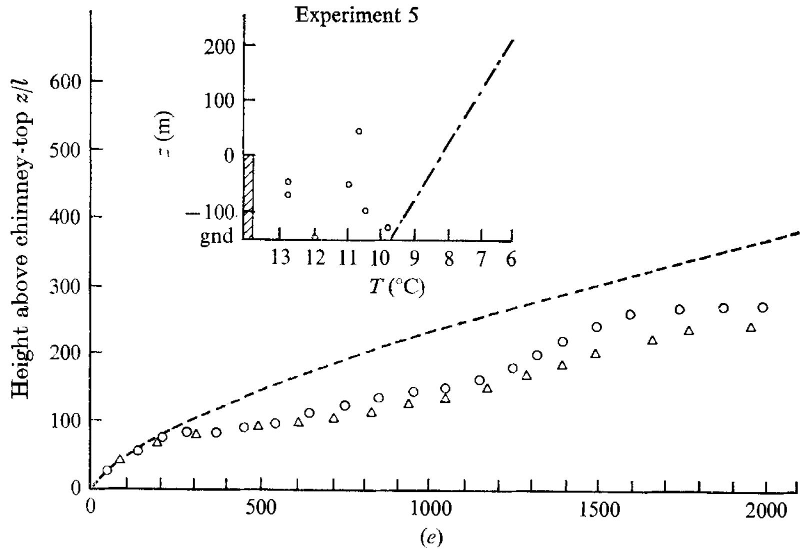

(*e*)

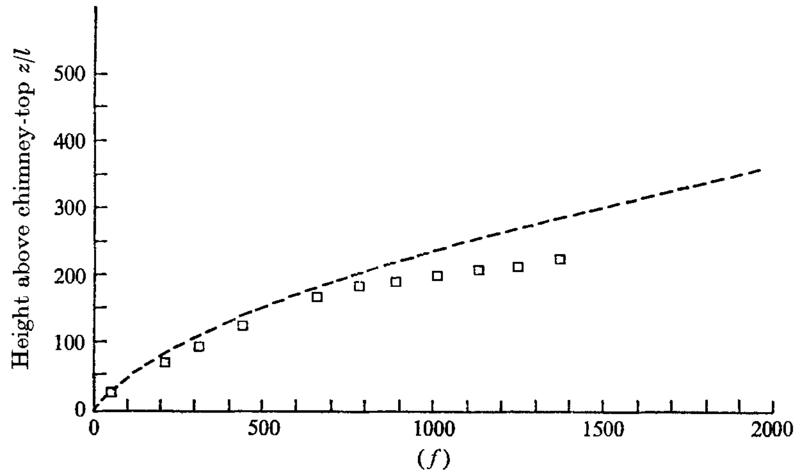

(*f*)

FIGURE 4 (*e*) and (*f*). For legend see p. 48.

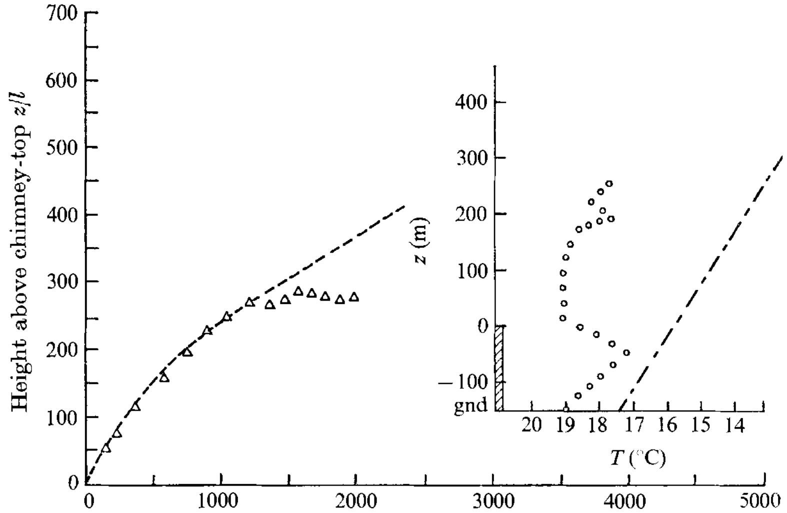

(g)

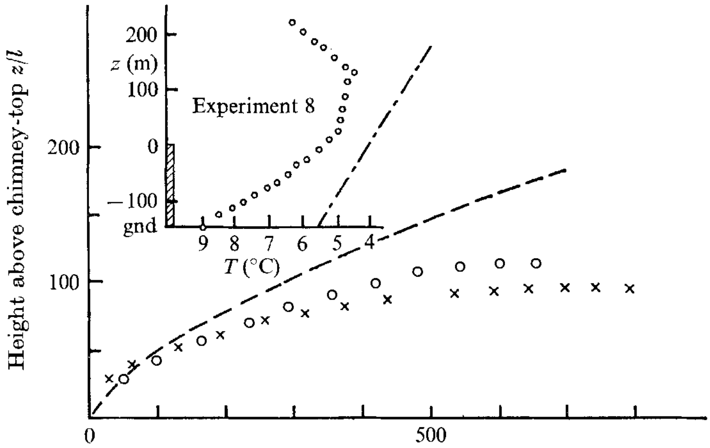

(h)

FIGURE 4. Plumes observed under various atmospheric stability conditions. – – –, $z/l = 2{\cdot}3(x/l)^{\frac{2}{3}}$.

	Expt. no.		l (m)	Date
(a)	12		0·429	19 May 1967
(b)	9		0·981	16 May 1967
(c)	10		0·999	17 May 1967
(d)	6		0·582	3 May 1967
(e)	5	○	0·62	2 April 1965
	5	△	0·71	27 April 1967
(f)	4		0·649	24 April 1967
(g)	11		0·695	18 May 1967
(h)	7	×	2·89	4 May 1967
	8	○	2·81	10 May 1967

Additional information for (e): symbols: ○, △; cloud cover: 0/10, 6/10; ceiling height: ——, 1219; mean wind direction: 346, 345; $\overline{U}$ (ft/sec) (m/sec): 9·8, 9·6; G_v: 0·0789, 0·071; G_h: 0·2496, 0·27.

The research reported here has been supported financially by the Meteorological Service of Canada and by the U.S. Atomic Energy Commission under contract no. NYO-3685. The authors are indebted to Dr R. E. Munn of the Meteorological Service of Canada for the loan of equipment and the time his group has freely given.

REFERENCES

BRIGGS, G. A. 1969 *Plume rise.* AEC Critical Review Series.

BRINGFELT, B. 1969 A study of buoyant chimney plumes in neutral and stable atmospheres. *Atm. Env.* **3**, 609–623.

CSANADY, G. T. 1965 The buoyant motion within a hot gas plume in a horizontal wind. *J. Fluid Mech.* **22**, 225.

HOULT, D. P., FAY, J. A. & FORNEY, L. J. 1969 A theory of plume rise compared with field observations. *J. Air Poll. Control Ass.* **19**, 585–590.

MOORE, D. J. 1966 Physical aspects of plume models. *Int. J. Air Water Poll.* **10**, 411.

MORTON, B. R., TAYLOR, G. I. & TURNER, J. S. 1956 Turbulent gravitational convection from maintained and instantaneous sources. *Proc. Roy. Soc.* A **23**, 1.

SLAWSON, P. R. 1968 On the mean path of buoyant bent-over plumes under various atmospheric stability conditions. *University of Waterloo, Mech. Eng. Report*, no. **13**.

SLAWSON, P. R. & CSANADY, G. T. 1967 On the mean path of buoyant, bent-over chimney plumes. *J. Fluid Mech.* **28**, 311–322.